WUSCHEL-related homeobox family genes in rice control lateral root primordium size

Tsubasa Kawai[a,b], Kyosuke Shibata[a], Ryosuke Akahoshi[a], Shunsaku Nishiuchi[a], Hirokazu Takahashi[a], Mikio Nakazono[a,b], Takaaki Kojima[a], Misuzu Nosaka-Takahashi[c], Yutaka Sato[c], Atsushi Toyoda[c], Nonawin Lucob-Agustin[a,d], Mana Kano-Nakata[e], Roel R. Suralta[d], Jonathan M. Niones[f], Yinglong Chen[b], Kadambot H. M. Siddique[b], Akira Yamauchi[a], and Yoshiaki Inukai[e,1]

[a]Graduate School of Bioagricultural Sciences, Nagoya University, Nagoya 464-8601, Japan; [b]The UWA Institute of Agriculture, and School of Agriculture and Environment, The University of Western Australia, Perth, WA 6009, Australia; [c]National Institute of Genetics, Mishima 411-8540, Japan; [d]Crop Biotechnology Center, Philippine Rice Research Institute, Science City of Muñoz 3119, Philippines; [e]International Center for Research and Education in Agriculture, Nagoya University, Nagoya 464-8601, Japan; and [f]Genetic Resource Division, Philippine Rice Research Institute, Science City of Muñoz 3119, Philippines

Edited by Luis Herrera-Estrella, Department of Plant and Soil Science, Texas Tech University, Lubbock, TX; received January 29, 2021; accepted November 3, 2021

The development of a plastic root system is essential for stable crop production under variable environments. Rice plants have two types of lateral roots (LRs): S-type (short and thin) and L-type (long, thick, and capable of further branching). LR types are determined at the primordium stage, with a larger primordium size in L-types than S-types. Despite the importance of LR types for rice adaptability to variable water conditions, molecular mechanisms underlying the primordium size control of LRs are unknown. Here, we show that two *WUSCHEL-related homeobox* (*WOX*) genes have opposing roles in controlling LR primordium (LRP) size in rice. Root tip excision on seminal roots induced L-type LR formation with wider primordia formed from an early developmental stage. *QHB/OsWOX5* was isolated as a causative gene of a mutant that is defective in S-type LR formation but produces more L-type LRs than wild-type (WT) plants following root tip excision. A transcriptome analysis revealed that *OsWOX10* is highly up-regulated in L-type LRPs. *OsWOX10* overexpression in LRPs increased the LR diameter in an expression-dependent manner. Conversely, the mutation in *OsWOX10* decreased the L-type LR diameter under mild drought conditions. The *qhb* mutants had higher *OsWOX10* expression than WT after root tip excision. A yeast one-hybrid assay revealed that the transcriptional repressive activity of QHB was lost in *qhb* mutants. An electrophoresis mobility shift assay revealed that *OsWOX10* is a potential target of QHB. These data suggest that QHB represses LR diameter increase, repressing *OsWOX10*. Our findings could help improve root system plasticity under variable environments.

lateral root primordium | root development | *WUSCHEL-related homeobox* genes | *Oryza sativa* L. | developmental plasticity

Root system development is highly plastic to spatiotemporal changes in soil resources. Soil water is distributed heterogeneously, and its availability and distribution change during crop cultivation period because of successive evaporation and precipitation (1). Climate change accelerates plant vulnerability to the adverse environments, with water deficiency becoming a more severe problem for sustainable crop production (2). In this context, improving root phenotypic plasticity, which is genetically regulated and heritable, is the key to better crop production with more efficient water acquisition (3).

Lateral roots (LRs) are produced postembryonically from main roots, including the seminal root (SR) and crown roots (CRs) in the case of rice, and play a major role in water and nutrient uptake. Recently, regulatory mechanisms underlying plastic LR formation have been studied in *Arabidopsis* and cereal plants (4). In plant roots, the auxin-regulated LR formation pathway is modulated in response to soil water distribution, determining whether—and in which direction—LRs form (5, 6). In rice, the plastic development of different types of LRs plays an important role in the adaptation to variable water stress conditions (7, 8). In rice and other cereals, LRs are classified as S-types or L-types according to distinct morphological and anatomical characteristics (9–12); S-type LRs are short and thin and do not produce higher-order LRs, whereas L-type LRs are long and thick and often produce higher-order LRs. L-type LR formation is promoted by water deficit and osmotic stress, contributing to root system expansion due to its higher branching ability (13–15). Rice genotypes with higher phenotypic plasticity of L-type LRs increase total root length in response to drought stress, thus maintaining dry matter production under mild drought conditions (13, 15).

LR type is determined at the primordium stage when an apical meristem with a distinct size is formed between L-types and S-types (9, 16). L-type LRs are more anatomically similar to main roots than S-types in terms of developed vascular structure and the presence of sclerenchyma and multiple cortex layers (10, 17, 18). The ability of LRs to produce higher-order LRs is related to their diameter, which is associated with internal structures such as the thickness of the cortical cell layers and stele (17, 18). The diameter of root apex is regarded as an

Significance

In recent years, phenotypic plasticity has received attention for improving plant adaptability to variable environments. For more than half a century, it has been known that rice and cereal plants develop different types of lateral roots (LRs), unlike the dicot model plant *Arabidopsis*. Despite the importance of plastic LR development under variable water conditions, the molecular mechanisms regulating LR types are unknown. Here, we report the regulatory mechanism of LR primordium size in rice, an important determinant of LR type. We identified two *WUSCHEL*-related homeobox (WOX) transcription factors that opposingly regulate LR primordium size. Our findings form the basis for improving root phenotypic plasticity for sustainable crop production under variable environments.

Author contributions: T. Kawai, M.N., Y.S., A.T., Y.C., K.H.M.S., A.Y., and Y.I. designed research; T. Kawai, K.S., R.A., S.N., H.T., T. Kojima, M.N.-T., N.L.-A., M.K-N., R.R.S., and J.M.N. performed research; T. Kawai, K.S., R.A., and Y.I. analyzed data; and T. Kawai and Y.I. wrote the paper.

The authors declare no competing interest.

This article is a PNAS Direct Submission.

[1]To whom correspondence may be addressed. Email: inukaiy@agr.nagoya-u.ac.jp.

This article contains supporting information online at http://www.pnas.org/lookup/suppl/doi:10.1073/pnas.2101846119/-/DCSupplemental.

Published December 30, 2021.

indicator of sink strength (19), and LR diameter is positively correlated with LR length (18). Recently, we isolated a rice mutant with promoted L-type LR formation, and the analysis of the mutant suggested the involvement of auxin in L-type LR formation (20). However, the molecular mechanisms underlying primordium size control of LRs are unclear.

The *WUSCHEL-related homeobox* (*WOX*) genes encode plant-specific homeodomain transcription factors. WOX transcription factors have important roles in determining cell fate and plant tissue development. In rice, 13 *WOX* genes were found in its genome (21). *QHB*/*OsWOX5* is the first characterized rice *WOX* gene involved in the specification and maintenance of stem cells in the root apical meristem (RAM) (22). *OsWOX11* positively regulates CR emergence and growth by the modulating of plant hormone signaling (23, 24). Other rice *WOX* genes are involved in maintaining shoot apical meristem and leaf and tiller development (25–27).

In a previous study, we established a method of root tip excision in SR, which promotes L-type LR formation in the remaining proximal portions of wild-type (WT) rice ("Taichung 65") (18). In this study, the mechanism of LR primordium (LRP) size control is studied through both forward and reverse genetics approaches with the root tip excision method. Root tip excision was used to screen mutants, and *QHB*/*OsWOX5* was detected as a causative gene of the mutant producing more L-type LRs in response to root tip excision. In addition, a transcriptome analysis between S- and L-type LRPs revealed that *OsWOX10* is highly up-regulated in L-type LRPs. Further analysis suggested that these two *WOX* genes play opposing roles in controlling LRP size in rice.

Results

Identification of a Mutant with a Defect in S-Type but Promoted L-Type LR Formation Following Root Tip Excision. A method of root tip excision in SR, which promotes L-type LR formation in the remaining proximal portions of WT rice ("Taichung 65") (Fig. 1 *A*–*C* and ref. 18), was applied to an *N*-methyl-*N*-nitrosourea (MNU)-mutagenized population to screen mutants with altered LR formation. A recessive mutant, T3-7–1, was isolated; this mutant developed fewer LRs, but new LRs emerged following root tip excision (Fig. 1 *D*–*G*). Interestingly, this recovery was observed in L-type LRs (≥150 μm in diameter) but not S-type LRs (<100 μm) or the intermediate type (Fig. 1 *H*–*J*). Notably, the mutant produced more L-type LRs than the WT following root tip excision, with increases in regions distant from the cut site (Fig. 1 *J* and *K*). This suggests that the causative gene of the T3-7–1 mutant represses the increase in LR diameter in regions distant from the cut site. Second-order LRs did not emerge from L-type LRs induced by root tip excision in the mutant; however, this defect in second-order branching was rescued by root tip excision in L-type LRs (*SI Appendix*, Fig. S1 *A*–*C*). Additionally, the mutant produced fewer CRs than the WT (*SI Appendix*, Fig. S1 *D* and *E*). Neither the length nor the gravitropic response in SRs changed in the T3-7–1 mutant (*SI Appendix*, Fig. S1 *F*–*I*). Thus, a causative gene of the T3-7–1 mutant was assumed to play a major role in developing CRs and S-type LRs, including second-order LRs, and repressing LR meristem enlargement in response to root tip excision (Fig. 1*L*).

We hypothesized that enhanced production of L-type LRs after root tip excision in the mutant was due to fewer CRs or LRs. Therefore, SRs were subjected to root tip excision in *crl1* and *Osiaa13* mutants, which produce fewer CRs and LRs, respectively (*SI Appendix*, Fig. S2 *A* and *B* and refs. 28 and 29). Consequently, both mutants produced similar numbers of L-type LRs compared with the WT after root tip excision (*SI Appendix*, Fig. S2 *C* and *D*). However, elongation of emerging LRs was enhanced in the mutants, including the T3-7–1 mutant (*SI Appendix*, Fig. S2*E*). Thus, the presence of fewer LRs and CRs may not be responsible for the increased number of L-type LRs in the T3-7–1 mutant.

Isolation of the Causative Gene of the T3-7–1 Mutant. We performed a linkage analysis of simple-sequence repeat markers to identify the causative gene of the T3-7–1 mutant using the 1,370 F_2 plants derived from a cross between the mutant and "Kasalath." The root phenotype of the mutant segregated in a 3:1 WT:mutant ratio. Map-based cloning revealed that the locus was located on chromosome 1 between RM11876 and RM3783 (~426 kb; Fig. 2*A*). This region contains about 40 genes including *QHB*/*OsWOX5* (*Quiescent center specific homeobox*; Os01g0854500; herein *QHB*). Comparing the WT and mutant sequences revealed a single-nucleotide substitution, from G to A, at the end of the intron in *QHB* (Fig. 2*B*). As the mutated site was likely to be important for splicing, the messenger RNA (mRNA) sequence was compared by synthesizing complementary DNA from the WT and mutant. The first nucleotide in the second exon was deleted in the mutant mRNA, resulting in a stop codon at the beginning of this exon (Fig. 2*C*). The introduction of a 4.7-kb genomic DNA fragment containing the entire *QHB* gene into the mutant complemented the mutant phenotype (*SI Appendix*, Fig. S3*A*). Thus, we concluded that the mutation in the *QHB* gene causes the mutant phenotype. Herein, the mutant is referred to as the *qhb* mutant. *QHB* is the first isolated *Wus*-type homeobox gene specifically expressed in the RAM of rice (22). *AtWOX5*, an orthologous gene in *Arabidopsis*, contains a WUS-box and an EAR motif in the C-terminal region, which confer repressive transcription factor activity (30). Both the WUS-box (TLE/QLFP) and EAR motif (P/LLE/DLRL) are well conserved among *QHB* orthologous genes from various plant species (*SI Appendix*, Fig. S3*B*). In the *qhb* mutant, a stop codon is present in front of the WUS-box and EAR motif (*SI Appendix*, Fig. S3*B*), suggesting that *qhb* may be a loss-of-function mutant.

Analysis of S- and L-Type LR Development in the WT and *qhb* Mutant. We analyzed the development of S-type LRs without root tip excision to determine the cause of reduction in S-type LRs in the *qhb* mutant. In the WT, the first anticlinal cell division was observed in pericycle cells ~5 mm from the SR tip (Fig. 2*D*). The LRP then underwent anticlinal and periclinal divisions, and the meristem was formed 24 h after initiation (Fig. 2*E* and *SI Appendix*, Fig. S4 *B*–*F*). Thereafter, S-type LRs continued to grow, emerging from the SRs within 36 h of initiation (Fig. 2*E* and *SI Appendix*, Fig. S4 *G* and *H*). No meristem formation was observed in the *qhb* mutant; smaller and deformed LRPs were observed 24 h after initiation (*SI Appendix*, Fig. S4*Q*). Among the LRPs observed 7 d after initiation in the *qhb* mutant, 20% stopped cell division after one round of anticlinal and periclinal divisions with irregular-shaped cells (Fig. 2 *F*, *Left*), and the remaining 80% had additional cell divisions with disturbed cellular organization (Fig. 2 *F*, *Right*) (n = 20 LRPs from five independent SRs). Furthermore, the LRs emerging from SRs were often short with a disorganized apical meristem (*SI Appendix*, Fig. S4*R*). Similar to S-type LR development, deformed CR primordia (CRPs) were found in mutant stems (*SI Appendix*, Fig. S5 *A*–*C*), consistent with *QHB* expression in CRPs (22).

Next, we analyzed L-type LR development in the WT and *qhb* mutant. The SR was cut 5 mm behind the root tip where the first anticlinal division was observed in the pericycle cell (Fig. 2*D*). A total of 6 h after root tip excision, LRP underwent an additional anticlinal division followed by periclinal division in pericycle cells and grew wider than the S-type with expanded cells (Fig. 2*G*). The expanded cells underwent anticlinal divisions in the L-type LRP 12 h after root tip excision (Fig. 2*G*), while pericycle cells in S-type underwent additional periclinal

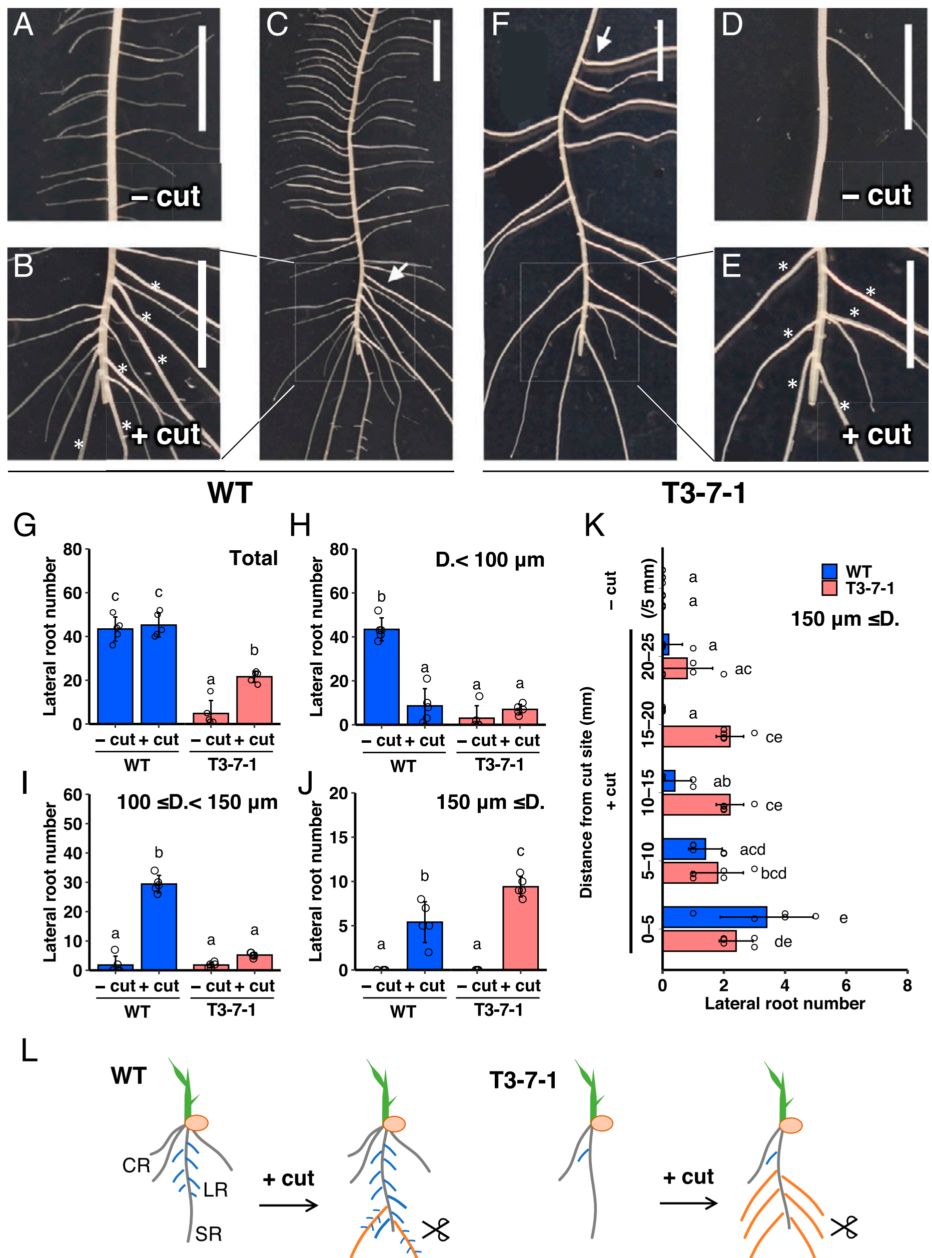

Fig. 1. Analysis of LR formation on SRs in the WT and T3-7–1 mutant. (*A*–*F*) Formation of LRs without (– cut) (*A* and *D*) or with (+ cut) root tip excision (*B*, *C*, *E*, and *F*) in WT (*A*–*C*) and T3-7–1 mutant (*D*–*F*) plants. Enlarged views of the boxed areas in *C* and *F* are shown in *B* and *E*, respectively. Asterisks indicate L-type LRs (*B* and *E*). Arrow indicates the L-type LR farthest from the cut site in each SR (*C* and *F*). (Scale bars, 5 mm.) (*G*–*J*), LR number in a region 0 to 25 mm from the cut site. Total number (*G*) and numbers in different diameter classes (*H*–*J*) are shown. (*K*) Number of L-type LRs in 5-mm sections 0 to 25 mm from the cut site. D., LR diameter. Bar plots show mean values ± SD (n = 5 independent biological replicates). Different lowercase letters indicate significant differences among groups (P < 0.05, multiple-comparison Tukey's test). (*L*) Schematic models of root phenotype in WT and T3-7–1 mutant.

divisions (Fig. 2*E*). Then, LRP underwent rounds of anticlinal and periclinal divisions, and the meristem formed 30 h after root tip excision (Fig. 2*G* and *SI Appendix*, Fig. S4 *L*–*N*), which was 6 h later than in S-type (Fig. 2*E*). The meristem was larger in L-type LRP with more cell layers in the ground tissue and stele than S-type (Fig. 2 *E* and *G*). In the *qhb* mutant, L-type LRPs with expanded cells were observed 12 h after root tip excision (Fig. 2*H*). L-type LR meristems with organized cell layers were established 30 h after root tip excision, similar to that in the WT (Fig. 2*H*). The sum of deformed LRPs and emerged LRs in the mutant was comparable with the number of LRs in the WT both without and with root tip excision (Fig. 2*L*). This suggests that QHB functions in meristem development but not in the initiation, and root tip excision recovers meristem formation of the initiated LRs of *qhb* mutants. Furthermore, the sum of CRPs and emerged CRs in the mutant was comparable to that in the WT (*SI Appendix*, Fig. S5*D*), suggesting that the function of QHB in meristem formation is conserved between S-type LRs and CRs.

We next analyzed *QHB* expression during S- and L-type LR development. *QHB* expression was first detected in pericycle cells at the initiation stage (Fig. 2*I* and *SI Appendix*, Fig. S6*A*). Thereafter, *QHB* expression was detected in whole LRP in both S- and L-types, with broader expression in the pericycle

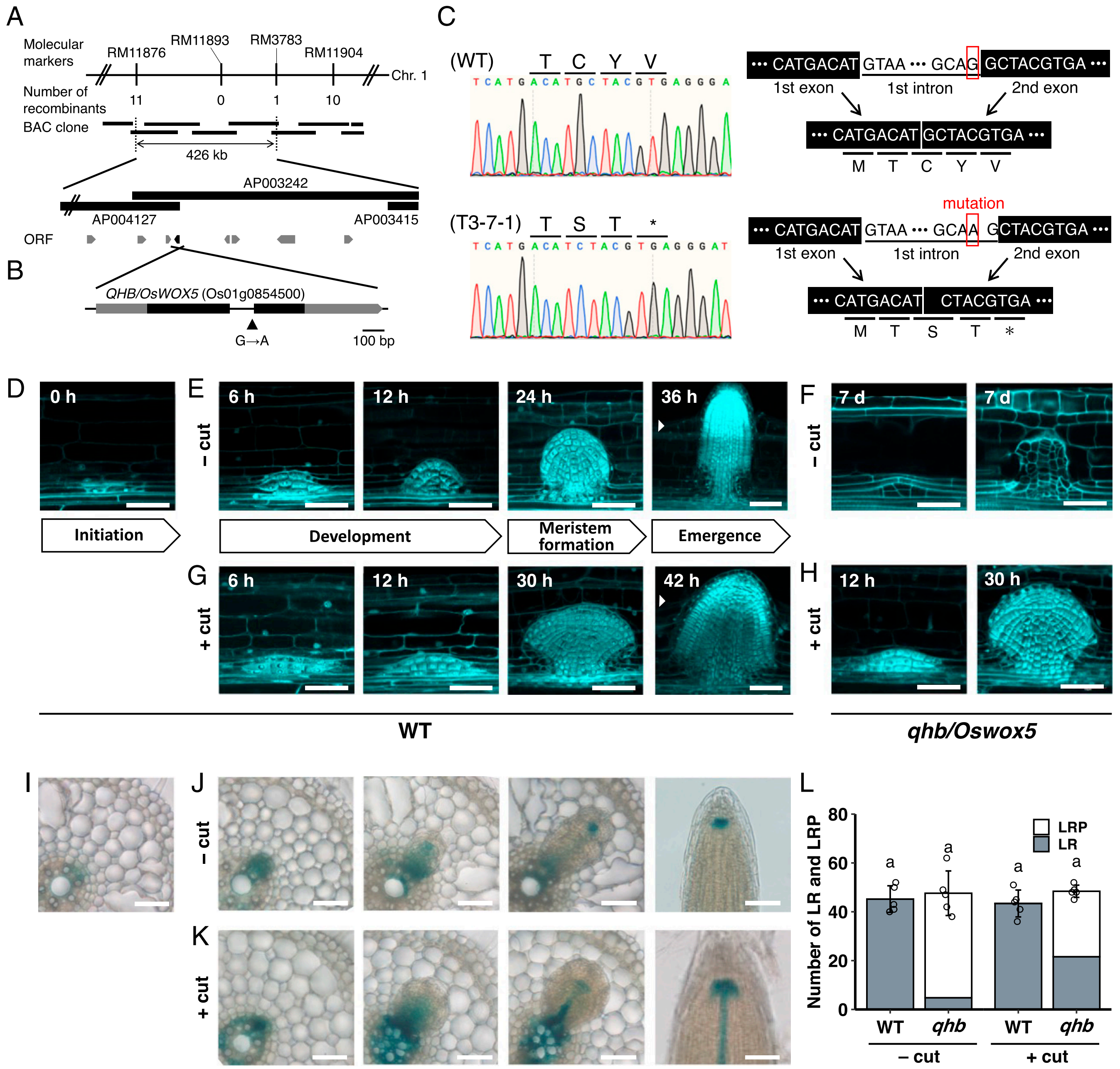

Fig. 2. Map-based cloning of the causative gene of the T3-7–1 mutant and its function in LR development. (*A*) High-resolution linkage and physical map of the causative gene locus on chromosome 1. The vertical bars represent molecular markers, and the numbers of recombinant plants are indicated below the linkage map. (*B*) Structure of the *QHB/OsWOX5* gene (Os01g0854500). Black and gray boxes indicate exons and untranslated regions, respectively. The arrowhead represents a single-nucleotide mutation in the intron at position 488 bp in the open reading frame. (*C*) The mutation site at the intron and resulting changes in splicing junction and amino acid sequence in the mutant. (*Left*) Sanger sequencing analysis around the splicing junction of *QHB* complementary DNA in the WT and *qhb* mutant. (*Right*) mRNA structures and amino acid sequences in WT and *qhb* mutant. (*D–H*) LR development in SR without (– cut) (*E* and *F*) or with (+ cut) root tip excision (*G* and *H*) in the WT (*D*, *E*, and *G*) and *qhb* mutant (*F* and *H*) plants. The first anticlinal division in pericycle cells was observed 5 mm behind the SR tip before root tip excision in the WT (*D*). Time after root tip excision is shown. (Scale bars, 50 μm.) Detailed development of WT plants is shown in *SI Appendix*, Fig. S4. (*I–K*), Expression of the *QHB* gene without (– cut) (*J*) or with (+ cut) root tip excision (*K*) during LR development observed in a cross-section of SR of *pQHB-GUS* in a WT background. Expression in the region 5 mm behind the root tip before root tip excision (*I*). (Scale bars, 50 μm.) (*L*) Comparison of the numbers of LRs and LR primordia in a region 0 to 25 mm from the cut site 7 d after root tip excision in the WT and *qhb* mutant. Values represent mean ± SD (n = 5 independent biological replicates). Different lowercase letters indicate significant differences among groups ($P < 0.05$, multiple-comparison Tukey's test).

cells of SRs with root tip excision (Fig. 2 *J* and *K* and *SI Appendix*, Fig. S6 *B*, *C*, *E*, and *F*). In S-type LRP, *QHB* expression was restricted to the quiescent center (QC) as meristem formation progressed (Fig. 2*J* and *SI Appendix*, Fig. S6*D*). Expression was similar in second-order LR formation on L-type LRs induced by root tip excision (*SI Appendix*, Fig. S6 *H–K*). In L-type LRP, *QHB* was expressed in late metaxylem (LMX) precursor cells and the QC after meristem formation (Fig. 2*K* and *SI Appendix*, Fig. S6*G*), similar to that in SRs (*SI Appendix*, Fig. S6*L* and ref. 31).

Identification of the Genes Differentially Expressed in S- and L-Type LRP. We next performed an RNA sequencing (RNA-seq) analysis of L-type LRPs isolated from SRs after 12 h of root tip excision and S-type LRPs of a similar developmental stage isolated from intact SRs in the WT, respectively. In total, 531 genes were up-regulated (259 genes) or down-regulated (272 genes) by more than twofold (adjusted $P < 0.05$) in L-type LRP than S-type (Fig. 3 *A* and *B* and Datasets S1 and S2). Gene ontology (GO) analysis revealed the enrichment of genes with common and different functions between up-regulated and down-regulated genes (Fig. 3*C*, *SI Appendix*, Figs. S7 and S8, and Datasets S3 and S4). In both groups, genes with "transcription regulator activity" were enriched (Fig. 3*C*). Enriched GO terms of "molecular function" were greater in up-regulated than down-regulated genes and included several terms related to oxidative stress (Fig. 3*C*), suggesting that the root tip excision triggers the wounding stress response in L-type LRP. Because L-type LRs are induced by auxin treatment (20), we explored the response of 259 up-regulated genes in response to auxin (32). A total of 73 of the 259 up-regulated genes in L-type LRP were auxin inducible in roots ($P < 0.05$, Fold change > 2, at least one time point after indole-3-acetic acid treatment compared with no treatment in the "root gene expression profile in response to auxin" microarray dataset [identification: RXP-1008], Dataset S1), which was significantly enriched among all genes ($P = 1.9\text{E-}15$, χ^2 test). The expression of *OsIAA9* and *20*, which are highly auxin-inducible *AUX*/*IAA* genes (33), were up-regulated in L-type LRP, which was confirmed by qRT-PCR (*SI Appendix*, Fig. S9). The most plausible hypothesis is that auxin accumulates in the proximal portions after root tip excision, causing L-type LR formation. To test this hypothesis, an SR after root tip excision was treated with a polar auxin transport inhibitor, *N*-1-naphthylphthalamic acid (NPA), in the WT. The NPA treatment resulted in a decrease in LR number

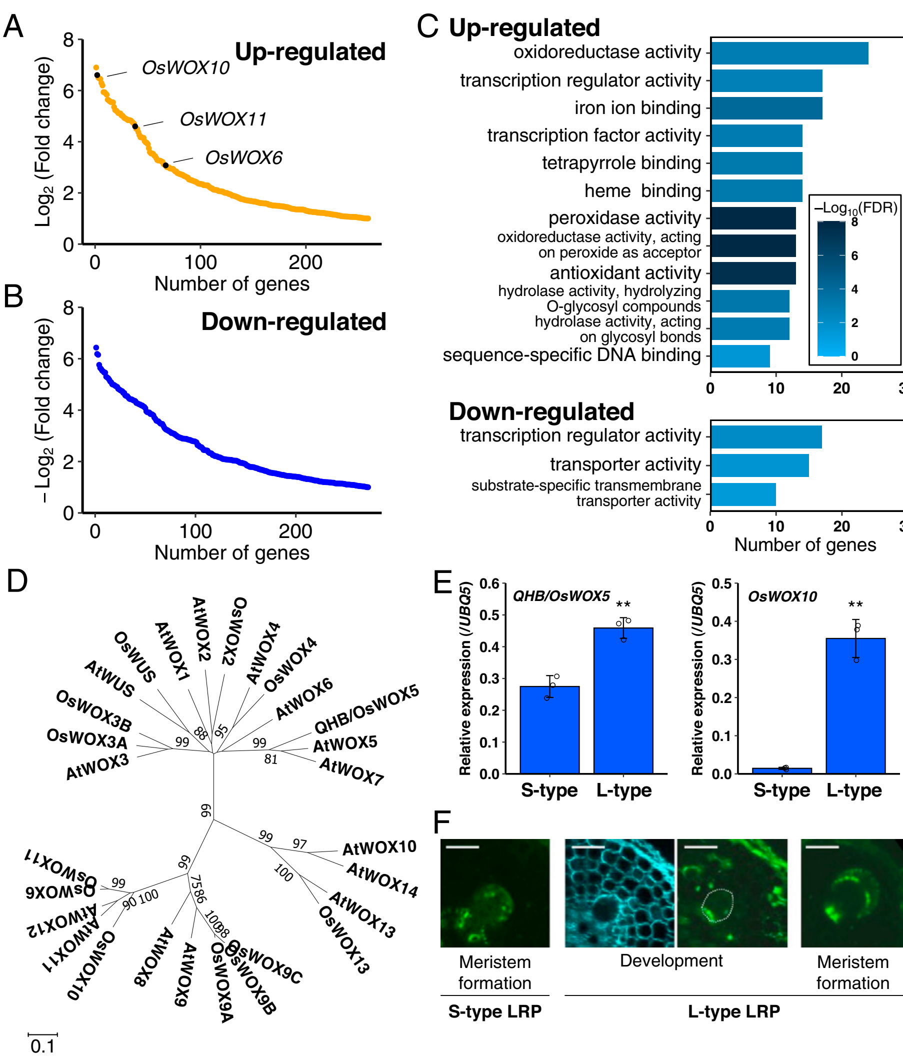

Fig. 3. Transcriptome analysis in S- and L-type LRPs. S- and L-type LRPs were isolated from SRs without and 12 h after root tip excision in the WT, respectively. (*A* and *B*) Logarithm fold changes in 259 up-regulated (*A*) and 272 down-regulated genes (*B*) presenting more than twofold changes in L-type LRP than S-type in the WT. (*C*) Enriched GO terms of "molecular function" in up-regulated and down-regulated genes in L-type LRP compared with S-type. (*D*) Phylogenetic tree constructed using the full-length amino acid sequences of WOX family proteins in rice and *Arabidopsis* using MEGA7. Numbers on branches are the 500 bootstrap values. Accession numbers of proteins are shown in *SI Appendix*, Table S4. (*E*) Relative expression levels of *QHB*/*OsWOX5* and *OsWOX10* in S- and L-type LRPs. Expression levels were quantified in S- and L-type LRPs isolated from SRs without and with 12 h of root tip excision, respectively. Values represent mean ± SD ($n = 3$ technical replicates, repeated with two biological replicates with similar results). Asterisks indicate significant differences between treatments (**$P < 0.01$, two-tailed Student's t test). (*F*) Promoter activity of *OsWOX10* visualized in T_0 transgenic plants containing *pOsWOX10-NLS-3xVENUS*. Expression in S- and L-type LRP developed in crown roots without (– cut) or with (+ cut) root tip excision, respectively. Green dots and blue color indicate *OsWOX10* expression and autofluorescence of cell walls, respectively. (Scale bars, 50 μm.)

in intact SRs in a dose-dependent manner; however, after both root tip excision and the treatment, a decrease in L-type LRs was not observed (*SI Appendix*, Fig. S10 *A* and *B*). In *Arabidopsis*, de novo auxin biosynthesis and auxin transport cooperatively increase LR number after root cutting (34). The application of an auxin biosynthesis inhibitor 5-(4-chlorophenyl)-4H-1, 2, 4-triazole-3-thio (Yucasin; ref 35) did not affect the L-type LR increase by root tip excision (*SI Appendix*, Fig. S10*D*), but the cotreatment of NPA and Yucasin suppressed L-type LR formation (*SI Appendix*, Fig. S10*F*), suggesting the synergistic regulation of L-type LR formation after root tip excision by auxin biosynthesis and transport.

Among 73 auxin-inducible genes up-regulated in L-type LRP, *OsWOX10* (Os08g0242400), a WOX domain transcription factor, was up-regulated to the greatest extent in L-type LRP (Fig. 3*A*). Notably, *OsWOX11* (Os07g0684900) and *OsWOX6* (Os03g0325600), homologous genes of *OsWOX10* clustered in the same clade among 13 rice WOX family proteins (Fig. 3*D*), were also up-regulated in L-type LRP (Fig. 3*A*). qRT-PCR detected slight up-regulation of *QHB*/*OsWOX5* in L-type LRP; however, the inclement was much higher in *OsWOX10* (Fig. 3*E*). Expression analysis with *pOsWOX10-NLS-3xVENUS* revealed that *OsWOX10* is expressed in the basal part of LRP from the early developmental stage in L-types and in the epidermal cell layer after meristem formation in both S- and L-types (Fig. 3*F*). Furthermore, several auxin-inducible genes encoding transcription factors that function as regulators of root development such as the *LATERAL ORGAN BOUNDARIES DOMAIN* (*LBD*) genes were also up-regulated in L-type LRP (*SI Appendix*, Fig. S9). Among them, *OsLBD2-1* (also named as *OsLOB16*; ref. 36) is the closest rice orthologous gene to *AtLBD16*, which is directly regulated by AtWOX11 and ARF7/19 and functions in LR formation (37, 38). Thus, *OsWOX10* and its homologous genes might play a major role in L-type LRP development.

***OsWOX10* Positively Affects LR Diameter Increase.** To analyze the functions of *OsWOX10* in LRP development, *OsWOX10* was overexpressed under the control of the *QHB* promoter to express it in the LRPs of intact SRs. *QHB* was expressed in S-type LRPs in intact SRs as well as L-types emerged after root tip excision (Fig. 2 *J* and *K*), while *OsWOX10* was not expressed in S-types at an early developmental stage (Fig. 3*F*). In a WT background, the number of L-type LRs in intact roots increased, while S-types and total LRs decreased under high *OsWOX10* expression (Fig. 4 *A*–*D* and *SI Appendix*, Fig. S11 *A* and *B*). Interestingly, the diameter of LRs increased in transgenic plants with increasing *OsWOX10* expression (Fig. 4*E* and *SI Appendix*, Fig. S11*C*). Notably, *pQHB-OsWOX10* did not rescue the reduced number of LRs in the intact roots of the *qhb* mutant (*SI Appendix*, Fig. S11 *D*–*F*). To verify the role of OsWOX10 in the control of LRP size, *Oswox10*-mutant

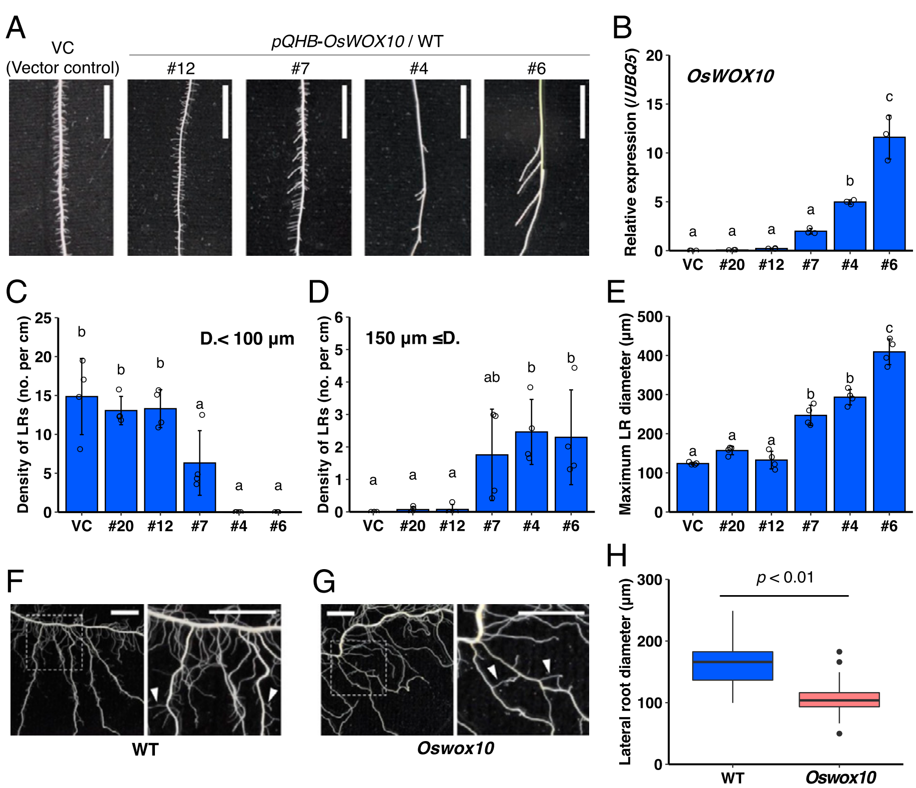

Fig. 4. Functional analysis of OsWOX10 in LR formation. (*A*) LR formation on CRs in T_0 transgenic plants containing *pQHB-OsWOX10* fusion DNA fragment in a WT background. (Scale bars, 1 cm.) (*B*–*E*) Relative expression levels of *OsWOX10* in CR tips (*B*) ($n = 3$ technical replicates), density of S- (*C*) and L-type LRs (*D*), and maximum LR diameter (*E*) ($n = 4$ independent biological replicates) in each transgenic line shown in *A*. VC, Vector control. D., LR diameter. Bar plots show mean values ± SD. Different lowercase letters indicate significant differences among groups ($P < 0.05$, multiple-comparison Tukey's test). (*F* and *G)* LR formation on CRs in the WT (*F*) and T_0 *Oswox10* mutant (*G*) grown in soils under mild drought stress condition. (*Right*) Enlarged views of the boxed areas. Arrow heads indicate second-order LRs. (Scale bars, 5 mm.) (*H*) Diameter of LRs with second-order LRs in *F* and *G*. Boxes show the first quartile, median, and third quartile. Whiskers show the range of nonoutlier values. Individual points indicate outlier values less than the first quartile or greater than the third quartile by 1.5 times the interquartile range. *P* value derived from two-tailed Student's *t* test ($n = 52$, 58 LRs from three independent CRs in WT and *Oswox10*, respectively).

Taichung 65 plants were generated using CRIPSR/Cas9 (*SI Appendix*, Fig. S11*G*). Under mild drought conditions, the WT produced LRs with higher-order branching, distinct from S-types in diameter and length (Fig. 4*F*). *Oswox10* mutants also produced LRs with higher-order branching; however, these LRs were significantly thinner than the WT (Fig. 4 *G* and *H*), verifying that OsWOX10 positively affects LR diameter.

As the *qhb* mutant produced more L-type LRs after root tip excision than WT (Fig. 1 *J* and *K*), we examined whether *OsWOX10* is differently regulated in WT and the mutant. qRT-PCR revealed that the increased *OsWOX10* expression, caused by root tip excision, gradually weakened with distance from the cut site in the WT (Fig. 5*A*), similar to the change in L-type LR number (Fig. 1*K*). *qhb* mutants had higher *OsWOX10* expression than the WT near the cut site, which was maintained at higher levels even in distant regions (Fig. 5*A* and *SI Appendix*, Fig. S11*H*), consistent with the formation of L-type LRs in distant regions in the mutant (Fig. 1*K*). *QHB* expression increased following root tip excision in the WT and mutant (Fig. 5*B* and *SI Appendix*, Fig. S11*I*); however, the mutant-type QHB might not be functional, resulting in a greater increase in *OsWOX10* expression in the mutant. As orthologous genes of both *OsWOX10* and *QHB* are up-regulated after wounding in leaf explants in *Arabidopsis* (39), it was assumed that the higher expression of *OsWOX10* in the *qhb* mutant was due to higher sensitivity to wounding stress in the mutant. The expression patterns of wounding stress marker genes, up-regulated in L-type LRP, were analyzed to test this hypothesis. As a result, no major differences between the WT and *qhb* mutant were detected in the tested genes (*SI Appendix*, Fig. S12), suggesting that wounding signaling level does not differ between the WT and *qhb* mutant.

Next, we tested the hypothesis that QHB negatively regulates *OsWOX10* expression, and thus, *OsWOX10* expression is higher in the *qhb* mutant than the WT after root tip excision. We first analyzed the transcriptional repressive activity of QHB, as the WUS-box and EAR motif, which confers repressive activity, are well conserved in QHB (*SI Appendix*, Fig. S3*B*). In the yeast one-hybrid assay, QHB suppressed the transcriptional activity of VP16 (Fig. 5*C*), suggesting the transcriptional repression of downstream genes. The mutant-type QHB protein, which lacks the WUS-box and EAR motif, did not suppress the activity of VP16 (Fig. 5*C*), suggesting that mutant-type QHB does not function as a transcriptional repressor. Next, we examined whether QHB directly binds to *OsWOX10* promoter regions. In the 1-kb upstream region of *OsWOX10*, we found two WOX-binding sequences (TTAATGG/C; refs. 22, 23, and 36) and nine core sequences (TAAT or its tandem repeat; refs. 30, 40, and 41). Among the nine core sequences, three were located near each other (from –320 to –283 base pair [bp] from the

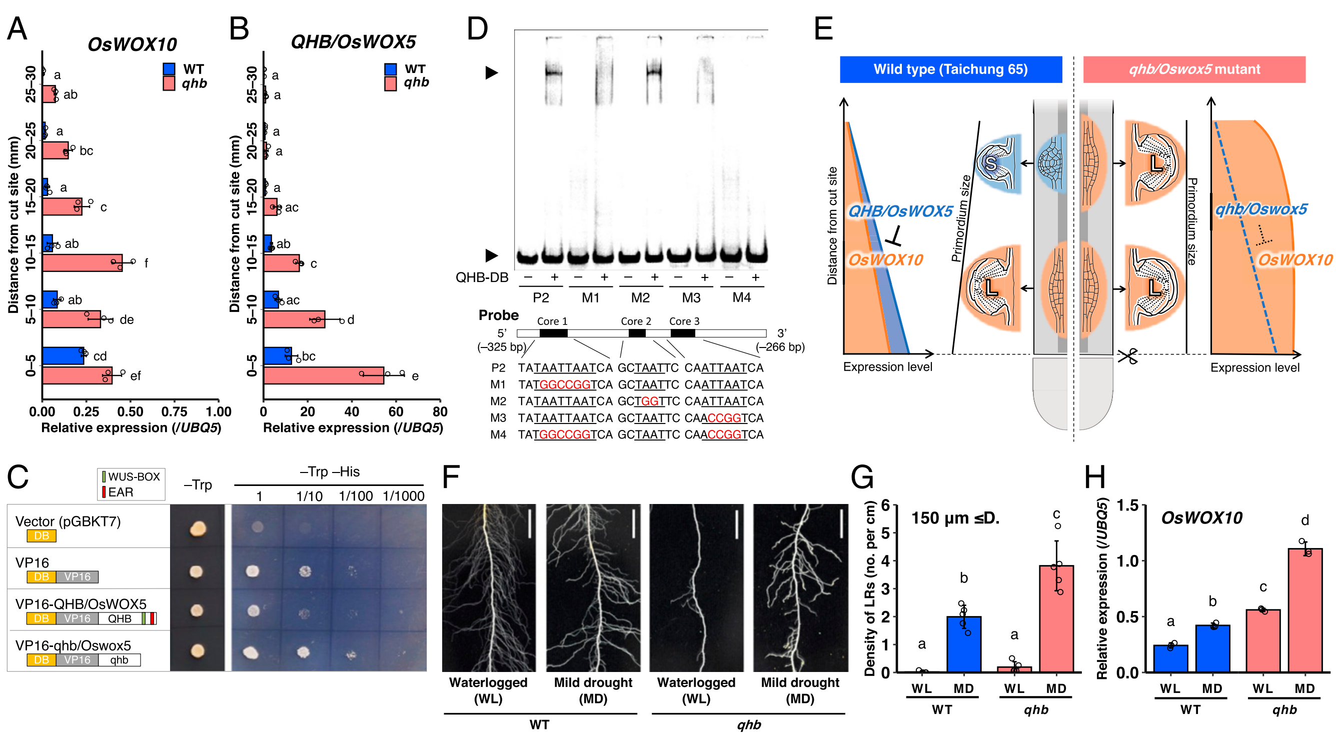

Fig. 5. Functional analysis of QHB/OsWOX5 as a negative regulator of *OsWOX10* expression. (*A* and *B*) Relative expression levels of *OsWOX10* (*A*) and *QHB/OsWOX5* (*B*) in the WT and *qhb* mutant. Expression levels were quantified in 5-mm SR sections 0 to 30 mm from the cut site 12 h after root tip excision (n = 3 technical replicates, repeated with two biological replicates with similar results). (*C*) Yeast one-hybrid assay to analyze the repressive activity of QHB/OsWOX5 of WT and *qhb* mutant versions. The serially diluted yeast cultures were spotted onto SD/–Trp and –Trp –His plates. (*Left*) Effector constructs. (*D*) Electrophoresis mobility shift assay of the recombinant DNA-binding domain (DB) of QHB/OsWOX5 and Cy5-labeled probes containing "TAAT" core sequences in *OsWOX10* promoter region. Upper and lower arrowheads indicate the shifted bands and free probes, respectively. (*Lower*) Sequences of probes with different mutation patterns in core sequences. The black boxes indicate the position of core elements in the probe. Underlined nucleotides show the core sequences, and red color indicates the mutated sequences. Base pairs in parentheses indicate the position in *OsWOX10* promoter (*QHB* translation start site: +1 bp). Full-length sequences of probes are shown in *SI Appendix*, Table S3. (*E*) Schematic models showing primordium size control of LRs regulated by QHB/OsWOX5 and OsWOX10. (*F*–*H*) LR formation on SRs in WT and *qhb* mutant grown in soils. Seedlings were grown under waterlogged (WL) and mild drought condition (MD) (20% [wt/wt] soil moisture content). (*F*) Formation of LRs. (Scale bars, 1 cm.) (*G*) Density of L-type LRs (≥150 µm in diameter) (n = 5 independent biological replicates). D., LR diameter. (*H*) Relative expression levels of *OsWOX10* quantified in seminal and crown roots 5 to 35 mm from root tip, containing developing LR primordia (n = 3 technical replicates). Bar plots show mean values ± SD. Different lowercase letters indicate significant differences among groups ($P < 0.05$, multiple-comparison Tukey's test).

https://doi.org/10.1073/pnas.2101846119

QHB translation start site); thus, it is more likely that QHB binds to this region. To test the binding of QHB to these candidate sequences, we performed an electrophoresis mobility shift assay (EMSA) with recombinant QHB proteins and Cy5-labeled DNA probes (P1–3, *SI Appendix*, Fig. S13*A*). The QHB bound to P2, containing three "TAAT" core sequences, but not to other probes (*SI Appendix*, Fig. S13*B*). As the shifted band in P2 was positioned higher than that in the positive control (intron of *Arabidopsis AGAMOUS* gene including "TTAA TGG"; ref. 22), it was assumed that QHB could target several "TAAT" core sequences in the P2 region. To verify which core sequences QHB binds to, we conducted EMSA with additional probes containing mutation(s) in the core sequences (Fig. 5*D*). As a result, shifted bands were not observed when Core 1 or 3 was mutated (Fig. 5*D*); thus, QHB binds to Core 1 and 3. These results suggest that *OsWOX10* is a potential target of QHB and negatively regulated by QHB.

To examine the regulation of LR diameter by QHB and OsWOX10 under soil conditions, the WT and *qhb* mutant seedlings were grown in soils with different water conditions, waterlogged and mild drought. Under mild drought, L-type LR number increased compared with waterlogged condition in the WT, with increased *OsWOX10* expression (Fig. 5 *F–H*). In the *qhb* mutant, *OsWOX10* expression and L-type LR number were higher than in WT under mild drought (Fig. 5 *F–H*). These observations suggest that QHB and OsWOX10 also control plastic LR development induced by mild drought in soil conditions.

Discussion

Based on this study's results, we provide models for primordium size control of LRs (Fig. 5*E*) and regulatory mechanisms for developing different LR types (*SI Appendix*, Fig. S14) in which QHB/OsWOX5 and OsWOX10 play different roles.

Mutant screening combined with the root tip excision method identified *QHB*/*OsWOX5* as a key regulator of root development in rice (Figs. 1 and 2 *A–C*). The *qhb* mutant was defective in developing S-type LRs, including second-order LRs, and CRs (Fig. 1 and *SI Appendix*, Fig. S1). In *Arabidopsis*, a mutation in *AtWOX5*, the orthologous gene of *QHB*, decreases LR density (42), but the detailed LRP phenotype of the *Atwox5* mutant has not been reported. During LR formation in *Arabidopsis*, *AtWOX5* expression is first detected in QC cells at the same time as QC is specified in the outer layer–derived cells (43), which is later than that in rice *QHB* detected just after LR initiation (Fig. 2 *I–K*). Therefore, *QHB* and *AtWOX5* might be involved in different steps of LR formation. The *qhb* mutant produced similar numbers of LRPs and CRPs to WT; however, cellular organization was disturbed in the primordia, decreasing the number of emerged S-type LRs and CRs (Fig. 2 *F* and *L* and *SI Appendix*, Fig. S5). In *Arabidopsis*, adventitious roots regenerated from leaf explants decreased in the *Atwox5 Atwox7* double mutant (*AtWOX7* is the homologous gene of *AtWOX5*) with root primordia formed but defective in cellular organization (39). Expressions of *AtWOX5* and *AtWOX7* were detected in the primordia after the transition of root founder cells to primordia in leaf explants of *Arabidopsis* (39). In rice CRs, *QHB* expression is first detected in the outer cell layer at the two-layer stage (22), which is as early as *AtWOX5* and *AtWOX7* expressions during adventitious rooting from leaf explants in *Arabidopsis* (39) and LR formation in rice (Fig. 2 *I–K*). These observations suggest that *QHB* and *AtWOX5* function in the cellular organization of root primordia in the root types in which they are expressed from the early developmental stage.

L-type LR development was recovered by root tip excision in the *qhb* mutant (Fig. 1), although *QHB* was expressed in both S- and L-type LRPs after initiation (Fig. 2 *I–K*). These data suggest that unknown factors might redundantly function in meristem formation of L-type LRs induced by root tip excision, but not S-type LRs. Notably, *OsWOX10* expression in LRP driven by the *QHB* promoter did not recover the defect in meristem formation in the *qhb* mutant (*SI Appendix*, Fig. S11 *D–F*); thus, other mechanisms might contribute to meristem formation of L-type LRs after root tip excision in the mutant (*SI Appendix*, Fig. S14). After meristem formation, *QHB* was expressed in the precursor cells of LMX and QC in L-type LRP (Fig. 2*K*). In SRs, decreased expression of *QHB* in LMX cells by the overexpression or exogenous treatment of FON2-LIKE CLE PROTEIN2 (FCP2p) impairs LMX development (31). *QHB* expression in LMX precursor cells of L-type LRPs may confer a more developed vascular structure of L-type LRs accompanied by an LMX and a larger number of proto xylems than S-types (10).

We revealed the opposing roles of two WOX transcription factors, QHB/OsWOX5 and OsWOX10, in the control of LRP size in rice (Fig. 5*E*). *OsWOX10* expression was positively correlated with LR diameter. In the WT, *OsWOX10* up-regulation by root tip excision gradually decreased with distance from the cut site (Fig. 5*A*) accompanied by a smaller L-type LR number in distant regions (Fig. 1*K*). Conversely, *OsWOX10* up-regulation was maintained in regions farthest from the cut site in *qhb* mutants (Fig. 5*A*), possibly increasing L-type LRs after root tip excision (Fig. 1 *J* and *K*). EMSA revealed that *OsWOX10* is a potential target of QHB (Fig. 5*D*), and thus, QHB may directly repress *OsWOX10* expression and the increase of LRP diameter. Notably, *OsWOX10* expression was not up-regulated in the *qhb* mutant than WT in intact SRs (*SI Appendix*, Fig. S11*H*). Since *OsWOX10* was not expressed in S-type LRPs before the meristem formation in the WT (Fig. 3*F*), it seems that up-regulation by a transcriptional activator is needed for *OsWOX10* expression in LRPs. As *OsWOX10* is an auxin-inducible gene and the auxin signaling is up-regulated in L-type LRPs than S-types (*SI Appendix*, Fig. S9), it is assumed that activation of auxin signaling and thus ARF transcription activity triggers *OsWOX10* expression in L-type LRPs. Both *QHB* and *OsWOX10* were induced in the SR sections after root tip excision (Fig. 5 *A* and *B*); however, the up-regulation of *OsWOX10* was much stronger than that of *QHB* in L-type LRPs (Fig. 3*E*). Therefore, *QHB* up-regulation after root tip excision may not be strong enough to completely repress *OsWOX10* expression near the cut site, resulting in *OsWOX10* up-regulation in L-type LRPs. It is noteworthy that S-type LRPs at early developmental stages can increase their LRP size and become L-types before the meristem is established (16, 18). The root cutting at different root positions revealed that early stage LRPs, which grow as S-type LRs, increase their diameter after root cutting and become L-type LR (16, 18). Further analyses are needed to clarify the function of QHB and OsWOX10 in this flexible regulation of LRP size.

The identified regulation of LR diameter by QHB and OsWOX10 would be involved in plastic LR development in soil conditions. *OsWOX10* expression increased with mild drought and possibly confers the increased L-type LRs under the condition in the WT (Fig. 5 *F–H*). In the *qhb* mutant, *OsWOX10* expression, hence L-type LR number, was higher than the WT under mild drought (Fig. 5 *F–H*). It is possible that the unidentified factor for meristem formation (discussed in the third paragraph) is absent in waterlogged conditions; thus, L-type LR number did not increase despite the higher *OsWOX10* expression in the *qhb* mutant than the WT under the condition. The mutation in *OsWOX10* decreased L-type LR diameter (LRs with second-order LRs) grown under mild drought conditions (Fig. 4 *F–H*). Interestingly, LRs in *Oswox10* plants grown under mild drought conditions produced higher-order branching despite the LR diameter decreasing (Fig. 4 *F–H*). This indicates that the thickness and higher branching ability of LRs, the characteristics used to determine LR types, are regulated by independent mechanisms. In *Arabidopsis*, the *Atwox11 Atwox12* double mutant produces LRs with fewer higher-order branches in soil than the WT (37), suggesting that WOX11/12 proteins differentially regulate the plastic LR development between rice and *Arabidopsis*.

In conclusion, our study reveals genetic mechanisms underlying primordium size control of LRs in rice. As the LR type determined by its primordium size is an important phenotypic trait for the growth maintenance of rice plants under variable water environments, our study provides important insights for improving plant resilience to environmental stresses through plastic root development.

Materials and Methods

Detailed information on plant material and growth conditions, root cutting treatments, chemical treatments, morphological characterization, histological characterization, map-based cloning, plasmid constructs, plant transformation, expression analysis, laser microdissection, RNA-seq analysis, yeast one-hybrid assay, electrophoresis mobility shift assay, and statistical analysis is provided in *SI Appendix, Materials and Methods*.

Data Availability. Transcriptome data have been deposited in DDBJ (DNA Data Bank of Japan; https://www.ddbj.nig.ac.jp/ddbj/index-e.html) (PRJDB11157; SAMD00276461–SAMD00276468). Gene expression profile was obtained at RiceXPro version 3.0 (https://ricexpro.dna.affrc.go.jp/, accessed on 4 October 2019).

ACKNOWLEDGMENTS. We thank Kimiyo Inukai, Eiko Murakami, and Saki Nishiuchi for their valuable technical support; Masafumi Mikami, Seiichi Toki, and Masaki Endo (National Agriculture and Food Research Organization) for providing the CRISPR–Cas9 vectors; Kotaro Miura for providing the screening lines for rice mutants; and Keisuke Nagai and Tokunori Hobo for providing the material for the yeast one-hybrid assay. This work was supported by the PRESTO program of the Japan Science and Technology Agency (JST) (15H04435), the SATREPS program (JPMJSA1706) of the JST and Japan International Cooperation Agency, and MEXT/JSPS KAKENHI (18H02174, 18J21800).

1. A. Kamoshita, R. C. Babu, N. M. Boopathi, S. Fukai, Phenotypic and genotypic analysis of drought-resistance traits for development of rice cultivars adapted to rainfed environments. *Field Crops Res.* **109**, 1–23 (2008).
2. M. Tester, P. Langridge, Breeding technologies to increase crop production in a changing world. *Science* **327**, 818–822 (2010).
3. A. B. Nicotra *et al.*, Plant phenotypic plasticity in a changing climate. *Trends Plant Sci.* **15**, 684–692 (2010).
4. H. Fromm, Root plasticity in the pursuit of water. *Plants* **8**, 236 (2019).
5. B. Orman-Ligeza *et al.*, The xerobranching response represses lateral root formation when roots are not in contact with water. *Curr. Biol.* **28**, 3165–3173 (2018).
6. B. Orosa-Puente *et al.*, Root branching toward water involves posttranslational modification of transcription factor ARF7. *Science* **362**, 1407–1410 (2018).
7. R. R. Suralta *et al.*, Root plasticity for maintenance of productivity under abiotic stressed soil environments in rice: Progress and prospects. *Field Crops Res.* **220**, 57–66 (2018).
8. N. Lucob-Agustin *et al.*, Morpho-physiological and molecular mechanisms of phenotypic root plasticity for rice adaptation to water stress conditions. *Breed. Sci.* **71**, 20–29 (2021).
9. S. Kawata, H. Shibayama, On the lateral root primordia formation in the crown roots of rice plant. *Proc. Crop Sci. Soc. Japan* **33**, 423–431 (1965).
10. Y. Kono, M. Igeta, N. Yamada, Studies on the developmental physiology of the lateral roots in rice seminal roots. *Proc. Crop Sci. Soc. Japan* **41**, 192–204 (1972).
11. A. Yamauchi, Y. Kono, J. Tatsumi, Quantitative analysis on root system structures of upland rice and maize. *Jpn. J. Crop. Sci.* **56**, 608–617 (1987).
12. A. Yamauchi, Y. Kono, J. Tatsumi, Comparison of root system structures of 13 species of cereals. *Jpn. J. Crop. Sci.* **56**, 618–631 (1987).
13. M. Kano, Y. Inukai, H. Kitano, A. Yamauchi, Root plasticity as the key root trait for adaptation to various intensities of drought stress in rice. *Plant Soil* **342**, 117–128 (2011).
14. K. Toyofuku, M. Matsunami, A. Ogawa, Genotypic variation in osmotic stress tolerance among rice cultivars and its association with L-type lateral root development. *Plant Prod. Sci.* **18**, 246–253 (2015).
15. D. M. Menge *et al.*, Drought-induced root plasticity of two upland NERICA varieties under conditions with contrasting soil depth characteristics. *Plant Prod. Sci.* **19**, 389–400 (2016).
16. O. Sasaki, K. Yamazaki, S. Kawata, The development of lateral root primordia in rice plants. *Jpn. J. Crop. Sci.* **53**, 169–175 (1984).
17. O. Sasaki, K. Yamazaki, S. Kawata, The relationship between the diameters and the structures of lateral roots in rice plants. *Jpn. J. Crop. Sci.* **50**, 476–480 (1981).
18. T. Kawai, M. Nosaka-Takahashi, A. Yamauchi, Y. Inukai, Compensatory growth of lateral roots responding to excision of seminal root tip in rice. *Plant Root* **11**, 48–57 (2017).
19. P. Thaler, L. C. Pagès, Why are laterals less affected than main axes by homogeneous unfavourable physical conditions? A model-based hypothesis. *Plant Soil* **217**, 151–157 (1999).
20. N. Lucob-Agustin *et al.*, *WEG1*, which encodes a cell wall hydroxyproline-rich glycoprotein, is essential for parental root elongation controlling lateral root formation in rice. *Physiol. Plant.* **169**, 214–227 (2020).
21. X. Zhang, J. Zong, J. Liu, J. Yin, D. Zhang, Genome-wide analysis of *WOX* gene family in rice, sorghum, maize, *Arabidopsis* and poplar. *J. Integr. Plant Biol.* **52**, 1016–1026 (2010).
22. N. Kamiya, H. Nagasaki, A. Morikami, Y. Sato, M. Matsuoka, Isolation and characterization of a rice *WUSCHEL*-type homeobox gene that is specifically expressed in the central cells of a quiescent center in the root apical meristem. *Plant J.* **35**, 429–441 (2003).
23. Y. Zhao, Y. Hu, M. Dai, L. Huang, D. X. Zhou, The WUSCHEL-related homeobox gene *WOX11* is required to activate shoot-borne crown root development in rice. *Plant Cell* **21**, 736–748 (2009).
24. T. Zhang *et al.*, The YUCCA-auxin-WOX11 module controls crown root development in rice. *Front Plant Sci.* **9**, 523 (2018).
25. J. Nardmann, W. Werr, The shoot stem cell niche in angiosperms: expression patterns of *WUS* orthologues in rice and maize imply major modifications in the course of mono- and dicot evolution. *Mol. Biol. Evol.* **23**, 2492–2504 (2006).
26. M. Dai, Y. Hu, Y. Zhao, H. Liu, D. X. Zhou, A *WUSCHEL-LIKE HOMEOBOX* gene represses a *YABBY* gene expression required for rice leaf development. *Plant Physiol.* **144**, 380–390 (2007).
27. W. Wang *et al.*, Dwarf Tiller1, a Wuschel-related homeobox transcription factor, is required for tiller growth in rice. *PLoS Genet.* **10**, e1004154 (2014).
28. Y. Inukai *et al.*, *Crown rootless1*, which is essential for crown root formation in rice, is a target of an AUXIN RESPONSE FACTOR in auxin signaling. *Plant Cell* **17**, 1387–1396 (2005).
29. Y. Kitomi, H. Inahashi, H. Takehisa, Y. Sato, Y. Inukai, OsIAA13-mediated auxin signaling is involved in lateral root initiation in rice. *Plant Sci.* **190**, 116–122 (2012).
30. L. Pi *et al.*, Organizer-derived WOX5 signal maintains root columella stem cells through chromatin-mediated repression of *CDF4* expression. *Dev. Cell* **33**, 576–588 (2015).
31. H. Chu *et al.*, A CLE-WOX signalling module regulates root meristem maintenance and vascular tissue development in rice. *J. Exp. Bot.* **64**, 5359–5369 (2013).
32. Y. Sato *et al.*, RiceXPro version 3.0: Expanding the informatics resource for rice transcriptome. *Nucleic Acids Res.* **41**, D1206–D1213 (2013).
33. Y. Song, L. Wang, L. Xiong, Comprehensive expression profiling analysis of *OsIAA* gene family in developmental processes and in response to phytohormone and stress treatments. *Planta* **229**, 577–591 (2009).
34. D. Xu *et al.*, *YUCCA9*-mediated auxin biosynthesis and polar auxin transport synergistically regulate regeneration of root systems following root cutting. *Plant Cell Physiol.* **58**, 1710–1723 (2017).
35. T. Nishimura *et al.*, Yucasin is a potent inhibitor of YUCCA, a key enzyme in auxin biosynthesis. *Plant J.* **77**, 352–366 (2014).
36. W. Jiang *et al.*, Transcriptional regulatory network of *WOX11* is involved in the control of crown root development, cytokinin signals, and redox in rice. *J. Exp. Bot.* **68**, 2787–2798 (2017).
37. L. Sheng *et al.*, Non-canonical *WOX11*-mediated root branching contributes to plasticity in *Arabidopsis* root system architecture. *Development* **144**, 3126–3133 (2017).
38. Y. Okushima, H. Fukaki, M. Onoda, A. Theologis, M. Tasaka, ARF7 and ARF19 regulate lateral root formation via direct activation of *LBD/ASL* genes in *Arabidopsis*. *Plant Cell* **19**, 118–130 (2007).
39. X. Hu, L. Xu, Transcription factors WOX11/12 directly activate *WOX5/7* to promote root primordia initiation and organogenesis. *Plant Physiol.* **172**, 2363–2373 (2016).
40. R. K. Yadav *et al.*, WUSCHEL protein movement mediates stem cell homeostasis in the *Arabidopsis* shoot apex. *Genes Dev.* **25**, 2025–2030 (2011).
41. R. K. Yadav *et al.*, Plant stem cell maintenance involves direct transcriptional repression of differentiation program. *Mol. Syst. Biol.* **9**, 654 (2013).
42. H. Tian, Y. Jia, T. Niu, Q. Yu, Z. Ding, The key players of the primary root growth and development also function in lateral roots in *Arabidopsis*. *Plant Cell Rep.* **33**, 745–753 (2014).
43. T. Goh *et al.*, Quiescent center initiation in the *Arabidopsis* lateral root primordia is dependent on the *SCARECROW* transcription factor. *Development* **143**, 3363–3371 (2016).